PROCEEDINGS OF SPIE

SPIEDigitalLibrary.org/conference-proceedings-of-spie

Energy landscape analysis of fMRI data from Schizophrenic and healthy subjects

Allen, Janerra, Varanasi, Sravani, Hong, Elliot, Choa, Fow-Sen

Janerra D. Allen, Sravani Varanasi, Elliot Hong, Fow-Sen Choa, "Energy landscape analysis of fMRI data from Schizophrenic and healthy subjects," Proc. SPIE 11756, Signal Processing, Sensor/Information Fusion, and Target Recognition XXX, 1175610 (12 April 2021); doi: 10.1117/12.2588046

SPIE.

Event: SPIE Defense + Commercial Sensing, 2021, Online Only

Energy landscape analysis of fMRI data from Schizophrenic and healthy subjects

Janerra D. Allen[a], Sravani Varanasi[b], Elliot Hong[c], Fow-Sen Choa[d*]

[a] University of Maryland, Baltimore County, 1000 Hilltop Circle, Baltimore MD 21250, USA
[b] University of Maryland, Baltimore County, 1000 Hilltop Circle, Baltimore MD 21250, USA
[c] University of Maryland, Baltimore, 620 West Lexington Street, Baltimore MD 21201, USA
[d] University of Maryland, Baltimore County, 1000 Hilltop Circle, Baltimore MD 21250, USA

ABSTRACT

Brain connectivity biomarkers are powerful tools for not only identifying neuropsychiatric disorders in patients but also validating treatment effectiveness. In this work, we used energy landscape techniques to analyze resting state fMRI data collected from 107 healthy control (HC) and 86 Schizophrenia patients (SZ). Activity patterns and disconnectivity graphs were obtained from 264 ROIs and 180-second fMRI time course of each subject. Statistics of individual and subgroups' inter-network and intra-network connections of Auditory Network (AUD), Attention Network (ATN), Default – Mode Network (DMN), Frontoparietal Network (FPN), Salience Network (SAN), Sensorimotor Network (SSM), and Visual Network (VIS) were analyzed. For inter-network results we found that the DMN and ATN of SZ are strongly coupled. But for HC, a stable brain states that the ATN, SAN, and FPN are coupled as a group and anti-correlated with the other coupled group of DMN, SSM, VIS, and AUD. For intra-networks we found that in FPN, controls have more flexibility to allow the Inferior Frontal Gyrus independently working together with the Superior Temporal Gyrus. In FPN we found that regions that process language and regions that process motor and planning can sometimes be decoupled in SZ. In SMN, some controls can accomplish a brain state to separate voluntary and autopilot activities. In VIS, controls have the ability to separate lower-level visual processing from working memory, motor planning, and guided coordination, whereas patients mixed some of them together, suggesting lack of self-awareness and self-constraint.

Keywords: energy landscape, fMRI, brain connectivity, biomarkers, Schizophrenia

1. INTRODUCTION

Functional magnetic resonance imaging (fMRI) is an effective tool used to study neural systems and functional connectivity patterns among brain structures (Rangaprakash, 2016; Subbaraju, 2017). FMRI helps uncover the functional differences in normal, diseased or injured brains, and mental disorders such as Schizophrenia (Rangaprakash, 2016; Subbaraju, 2017). In this study, we investigated brain activity differences in healthy controls (HC) and schizophrenic (SZ) patients in order to understand the work of each brain network involved. The differences in structural and functional behavior between SZ and HC could be attributed to inter-network and intra-network activity (Fan, 2016). Local minima were identified as potential biomarkers between patients and controls. This paper discusses the role of flexibility and stability in brain states within coupled networks.

1.1 Role of Intra-Networks

The intra-networks found in the Attention Network (ATN): Middle Frontal Gyrus (MFG), Inferior Frontal Gyrus (IFG), Superior Temporal Gyrus (STG), and Middle Temporal Gyrus (MTG) correspond with cognitive control, semantic decisions, perception of sound, and facial recognition, respectively (Koyama, 2017; Sundermann & Pfleiderer, 2012; Buchsbaum, 2010; Davey, 2016). More specifically, MFG corresponds to working memory, task switching, inhibitory control, short-term memory, inductive reasoning and planning. The IFG is involved in word association and representation

* Further author information: (Send correspondence to J.D.A.)
J.D.A.: E-mail: j178@umbc.edu, Telephone: 1 410 455 3272
S.V.: E-mail: sravani1@umbc.edu, Telephone: 1 410 455 3272

Signal Processing, Sensor/Information Fusion, and Target Recognition XXX, edited by Ivan Kadar,
Erik P. Blasch, Lynne L. Grewe, Proc. of SPIE Vol. 11756, 1175610 · © 2021 SPIE
CCC code: 0277-786X/21/$21 · doi: 10.1117/12.2588046

(Sundermann & Pfleiderer, 2012). The STG corresponds with the physical properties of pitch and sound intensity, in addition to understanding the meaning of words (Buchsbaum, 2010). The MTG is involved in recognizing faces (Acheson & Hagoort, 2013).

The STG and posterior Superior Temporal Sulcus (pSTS) intra-networks are found in the Auditory Network (AUD). The pSTS is responsible for recognizing movement and processing speech (Hocking & Price, 2008). It also corresponds with visual gaze and social cues (Hocking & Price, 2008). The "TE1.0 is particularly affected by high frequency hearing loss and may be a target for evaluating the efficacy of interventions for hearing loss. TE1.2 is associated with low frequency hearing" (Eckert, 2012). There is correlation between AUD and ATN inter-networks because of the STG region. In addition to the MFG and IFG regions, the Inferior Parietal Lobule (IPL) is included in the Frontoparietal Network (FPN). The IPL is primarily responsible for body image and perception (Torrey, 2007). IPL is also involved in word processing and phonology of texts (Baldo & Dronkers, 2006). There is correlation between ATN and ATN inter-networks because of the MFG and IFG regions.

The Sensorimotor Network (SSM) contains the following regions: Superior Frontal Gyrus (SFG), Precentral Gyrus (PrG), Paracentral Lobule (PCL), Superior Parietal Lobe (SPL), Postcentral Gyrus (PoG), and Cingulate Gyrus (CG). The SFG is responsible for self-awareness and laughter (Pollatos, 2007). The PrG is involved in executing voluntary motor movements (Yousry, 1997). The PCL controls motor and sensory innervations of the contralateral lower extremity (Torres & Beardsley, 2019). It is also responsible for control of defecation and urination (Radziunas, 2018). The SPL is responsible for spatial orientation (Kamali, 2014). The PoG is the main sensory receptive area for the sense of touch (Preusser, 2015). The CG is involved with emotion formation and processing, learning, and memory (Vogt, 2005) These functions combined makes the CG highly influential in linking motivational outcomes to behavior (Pujol, 2002; Posner, 2007).

The Visual Network (VIS) comprises of the Fusiform Gyrus (FuG), Medio Ventral Occipital Cortex (MVOcC), Lateral Occipital Cortex (LOcC) regions. The FuG is located in the temporal lobe region and plays a part in high-level visual processing and recognition memory (Fliessbach, 2006). Specifically, the FuG is responsible for processing color, face and body recognition, word and number recognition (Devlin, 2006). The MVOcC is located in the calcarine sulcus and the posterior part of the collateral sulcus of the occipital lobe (Wade, 2002; Astafier, 2004). MVOcC region is responsible for visual processing, dreaming, and encoding of complex images (Wade, 2002; Astafier, 2004). The lingual gyrus of the MVOcC processes whole shapes, and not the individual components of a shape (Wade, 2002; Astafier, 2004; Tosoni, 2015).

The LOcC region is primarily responsible for object recognition, (Grill-Spector, 2001; Silvanto, 2010). The LOcC comprises of the following areas: Middle Occipital Gyrus (MOccG), area V5/MT+, Occipital Polar Cortex (OPC), Inferior Occipital Gyrus (iOccG), Medial Superior Occipital Gyrus (msOccG), Lateral Superior Occipital gyrus (lsOccG). The MOccG showed that it was activated more during spatial than nonspatial tactile and auditory tasks. Visual area V5/MT+ would respond to all dynamic stimuli indiscriminately, given its sensitivity to visual motion cues (Malach, 1995; Tootell, 1995; Huk & Dougherty, 2002). The inferior occipital gyrus (iOccG) has been found to be related to the visual function of processing faces. The iOccG is connected to the amygdala via white matter connectivity. This allows the iOccG to form a network for facial recognition with the amygdala. The lateral superior occipital gyrus (lsOccG) is part of the dorsal extrastriate cortex implicated in higher level visual association processes, as a part of the visual dorsal stream (Uddén, 2017). Uddén et al (2017) suggests that problems with coordination, gait, balance and posture are due to impairment in motion detection and visually guided action processing located in the visual dorsal stream (Uddén, 2017).

2. MATERIALS AND METHODS

2.1 Data Preprocessing

We collected resting state fMRI data of 107 HC and 86 SZ. MR data was collected on a GE 1.5 T scanner with an eight-channel head coil. The resting-state data used for this study was preprocessed by the Maryland Psychiatric Research Center (MPRC) at the University of Maryland School of Medicine (UMSOM).

Table 1: Subnetwork affiliations parceled into inter-network and intra-network connectivity.

Network	Gyrus	Number	Architecture
ATN	MFG, Middle Frontal Gyrus	1	*left*, ventrolateral area 6
		2	*right*, ventrolateral area 6
	IFG, Inferior Frontal Gyrus	3	*left*, rostral area 45
		4	*right*, rostral area 45
	STG, Superior Temporal Gyrus	5	*left*, area 41/42
		6	*right*, area 41/42
	MTG, Middle Temporal Gyrus	7	*left*, dorsolateral area 37
		8	*right*, dorsolateral area 37
AUD	STG, Superior Temporal Gyrus	1	*left*, TE1.0 & TE1.2
		2	*right*, TE1.0 & TE1.2
		3	*left*, caudal area 22
		4	*right*, caudal area 22
		5	*left*, rostral area 22
		6	*right*, rostral area 22
	pSTS, posterior Superior Temporal Sulcus	7	*left*, rostro pSTS
		8	*right*, rostro pSTS
		9	*left*, caudo pSTS
		10	*right*, caudo pSTS
DMN	SFG, Superior Frontal Gyrus	1	*gyrus*, SFG
	MFG, Middle Frontal Gyrus	2	*gyrus*, MFG
	STG, Superior Temporal Gyrus	3	*gyrus*, STG
	MTG, Middle Temporal Gyrus	4	*gyrus*, MTG
	PhG, Parahippocampal Gyrus	5	*gyrus*, PhG
	IPL, Inferior Parietal Lobule	6	*gyrus*, IPL
	Pcun, Precuneus	7	*gyrus*, Pcun
	CG, Cingulate Gyrus	8	*gyrus*, CG
FPN	MFG, Middle Frontal Gyrus	1	*left & right*, inferior frontal junction
		2	*left & right*, ventral area 9/46
		3	*left & right*, lateral area 10
	IFG, Inferior Frontal Gyrus	4	*left & right*, dorsal area 44
		5	*left & right*, inferior frontal sulcus
	IPL, Inferior Parietal Lobule	6	*left & right*, rostrodorsal area 39
		7	*left & right*, rostrodorsal area 40
		8	*left & right*, caudal area 40
SAN	MFG, Middle Frontal Gyrus	1	*left & right*, area 46
	IFG, Inferior Frontal Gyrus	2	*left & right*, caudal area 45
		3	*left & right*, opercular area 44
		4	*left & right*, ventral area 44
	INS, Insular Gyrus	5	*left & right*, ventral agranular insula
		6	*left & right*, dorsal agranular insula
		7	*left & right*, dorsal granular insula
	CG, Cingulate Gyrus	8	*left & right*, pregenual area 32
		9	*left & right*, caudodorsal area 24
SSM	SFG, Superior Frontal Gyrus	1	*gyrus*, SFG
	PrG, Precentral Gyrus	2	*gyrus*, PrG
	PCL, Paracentral Lobule	3	*gyrus*, PCL
	SPL, Superior Parietal Lobule	4	*gyrus*, SPL
	PoG, Postcentral Gyrus	5	*gyrus*, PoG
	CG, Cingulate Gyrus	6	*gyrus*, CG
VIS	FuG, Fusiform Gyrus	1	*left & right*, rostroventral area 20
		2	*left & right*, medioventral area 37
		3	*left & right*, lateroventral area 37
	MVOcC, Medio Ventral Occipital Cortex	4	*left & right*, rostral & caudal lingual gyrus
		5	*left & right*, rostral & caudal cuneus gyrus
		6	*left & right*, ventromedial parietooccipital sulcus
	LOcC, lateral Occipital Cortex	7	*left & right*, middle & inferior occipital gyrus
		8	*left & right*, area V5/MT+
		9	*left & right*, occipital polar cortex
		10	*left & right*, medial & lateral superior occipital gyrus

2.2 Brainnetome

Brain-connectivity analysis requires a clear and accurate definition of brain network regions, which we achieved using the Brainnetome Atlas, a connectivity-based parcellation framework that contains information on anatomical and functional connections. We used 3D coordinates and subnetwork affiliations from the 264 ROI Power atlas and 90 ROI Automated Anatomical Labeling (AAL) atlas respectively, to align the Brainnetome atlas containing 246 voxels or subregions to 7 brain networks (Fan, 2016). The Energy Landscape toolbox interpreted brain activity of inter-network and intra-network connections among the 7 networks, including: ATN, AUD, DMN, FPN, SAN, SSM, and VIS. This was interpreted based on the properties and functions of each brain region and subsequent network brain network.

2.3 Energy Landscape

The energy landscape is an analysis tool used to calculate and interpret multivariate time series data (Ezaki, 2017). The energy landscape is achieved by (1) binarization of the data, (2) maximum entropy model (Boltzmann distribution) estimation, (3) disconnectivity graph and basin of energy local minima, (4) dynamics of energy landscapes (Ezaki, 2017). We constructed activity patterns and disconnectivity graphs for each subject using the Energy Landscape toolbox to interpret multivariate fMRI data.

The Boltzmann distribution is denoted by

$$P(\boldsymbol{\sigma} \mid \boldsymbol{h}, \mathbf{J}) = \frac{\exp[-E(\boldsymbol{\sigma} \mid \boldsymbol{h}, \mathbf{J})]}{\sum_{\boldsymbol{\sigma}'} \exp\left[-E\left(\boldsymbol{\sigma}' \middle| \boldsymbol{h}, \mathbf{J}\right)\right]'} \tag{1}$$

with Energy, E

$$E(\boldsymbol{\sigma} \mid \boldsymbol{h}, \mathbf{J}) = \sum_{i=1}^{N} h_i \sigma_i - \frac{1}{2} \sum_{i=1}^{N} \sum_{\substack{j=1 \\ j \neq i}}^{N} J_{ij}\, \sigma_i \sigma_j \tag{2}$$

and maximum likelihood

$$(\boldsymbol{h}, \mathbf{J}) = \arg\max_{\boldsymbol{h}, \mathbf{J}} \mathcal{L}\,(\boldsymbol{h}, \mathbf{J}) \tag{3}$$

with likelihood, $\mathcal{L}(\boldsymbol{h}, \mathbf{J})$

$$\mathcal{L}(\boldsymbol{h}, \mathbf{J}) \; = \prod_{t=1}^{t_{max}} P(\boldsymbol{\sigma}(t) \mid \boldsymbol{h}, \mathbf{J}) \tag{4}$$

2.4 Local Minima

The local minima are states that have lower energy (more frequent) relative to their neighboring nodes, N. Two minima are in different sets if the highest energy transitions state (a local maxima) or lowest energy pathway between them exceeds energy, E (Ezaki, 2017). The number of local energy minima (attractor states) is estimated and the disconnectivity graph shows the positions of the local minimum states and their relationships (Ezaki, 2017). The numbers on the x-axis of the activity patterns and disconnectivity graphs labeling the energy local minimum states are consistently used in both panels. White and black cells represent that variables (ROIs) are active (+1) and inactive (–1).

3. RESULTS

The following results are taken along the inter-network and intra-network regions. Each network was averaged in accordance with the Brainnetome cortical and subcortical region allocation. The controls tend to have more states than the patients, with the exception of the FPN and VIS intra-network calculations. The number of local minima vary between and controls and have been identified as biomarkers.

3.1 Local Minima as Potential Biomarkers

The internetwork results indicate that HC have 4 states that have been identified as local minima, whereas SZ has 2 states identified as local minima. For the ATN region, HC have 5 states that have been identified as local minima, whereas SZ has 4 states identified as local minima. There are 6 identifiable states that are local minima in the AUD region for both SZ and HC subjects. There are 2 identifiable states that are local minima in the DMN region for both SZ and HC subjects. For the FPN region, HC have 3 states that have been identified as local minima, whereas SZ has 4 states identified as local

3.1.1 Intra-Network Results

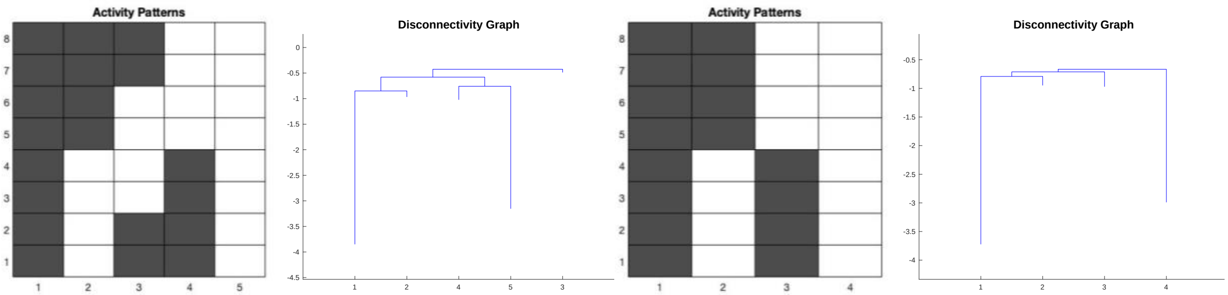

(a) **(b)**

Figure 1: Activity Patterns and Disconnectivity Graph for ATN of (**a**) all the averaged controls (**b**) all the averaged patients.

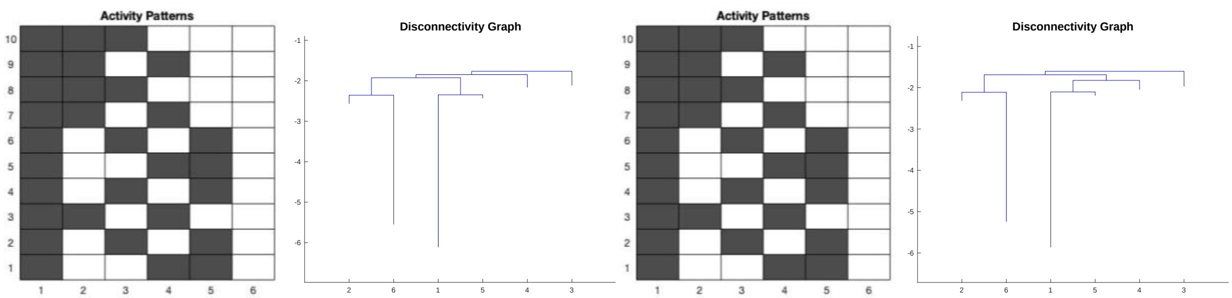

(a) **(b)**

Figure 2: Activity Patterns and Disconnectivity Graph for AUD of (**a**) all the averaged controls (**b**) all the averaged patients.

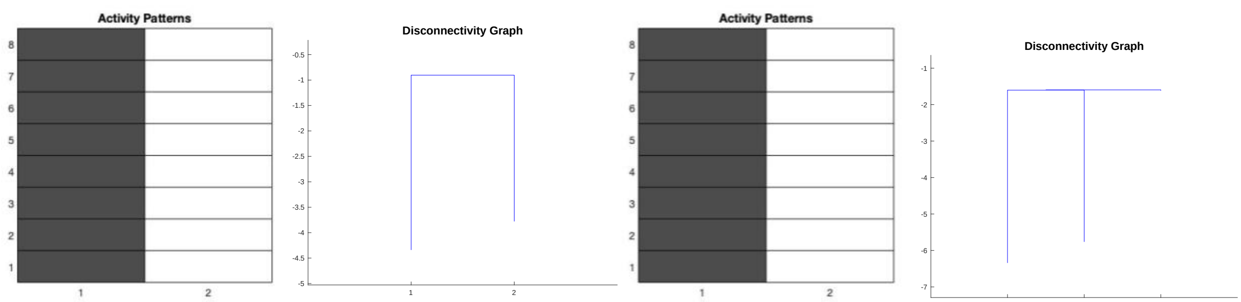

(a) **(b)**

Figure 3: Activity Patterns and Disconnectivity Graph for DMN of (**a**) all the averaged controls (**b**) all the averaged patients.

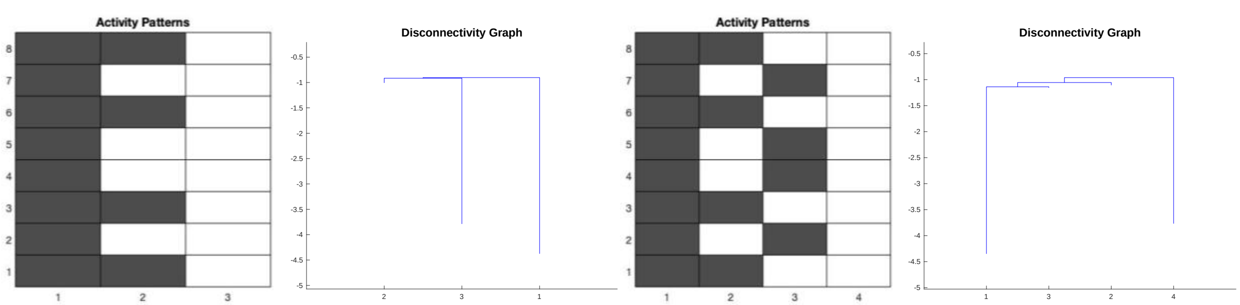

(a) **(b)**

Figure 4: Activity Patterns and Disconnectivity Graph for FPN of (**a**) all the averaged controls (**b**) all the averaged patients.

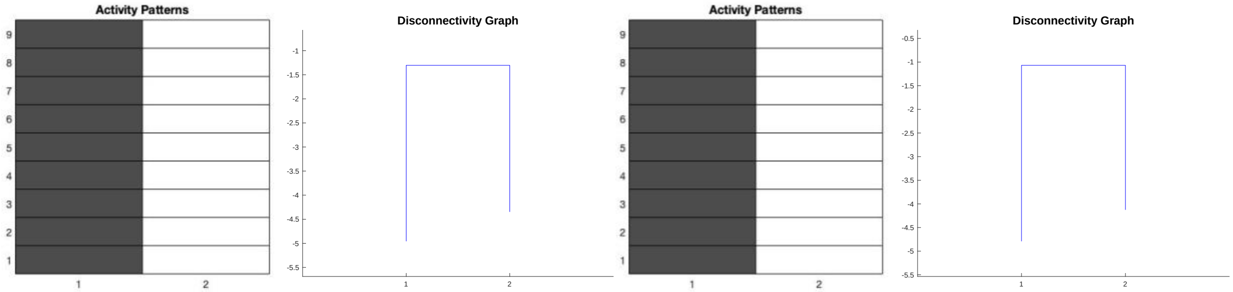

(a) **(b)**

Figure 5: Activity Patterns and Disconnectivity Graph for SAN of **(a)** all the averaged controls **(b)** all the averaged patients

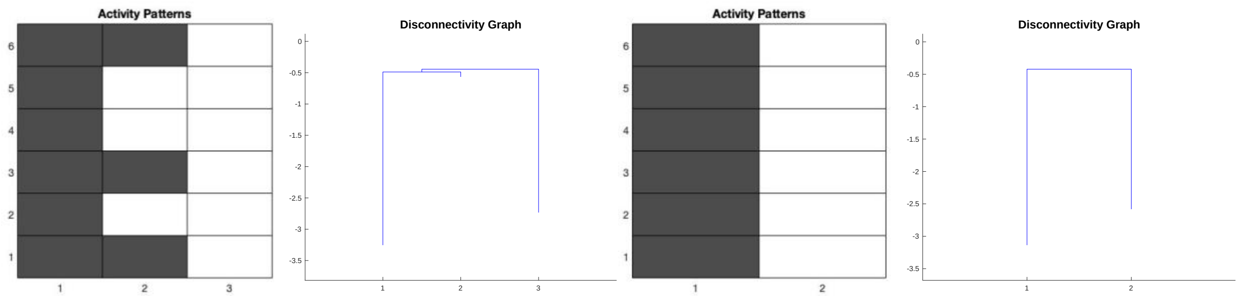

(a) **(b)**

Figure 6: Activity Patterns and Disconnectivity Graph for SSM of **(a)** all the averaged controls **(b)** all the averaged patients

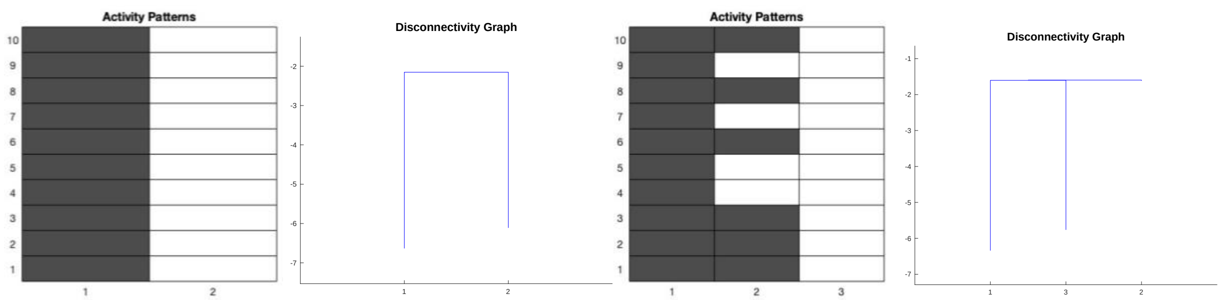

(a) **(b)**

Figure 7: Activity Patterns and Disconnectivity Graph for VIS of **(a)** all the averaged controls **(b)** all the averaged patients

3.1.2 Inter-Network Results

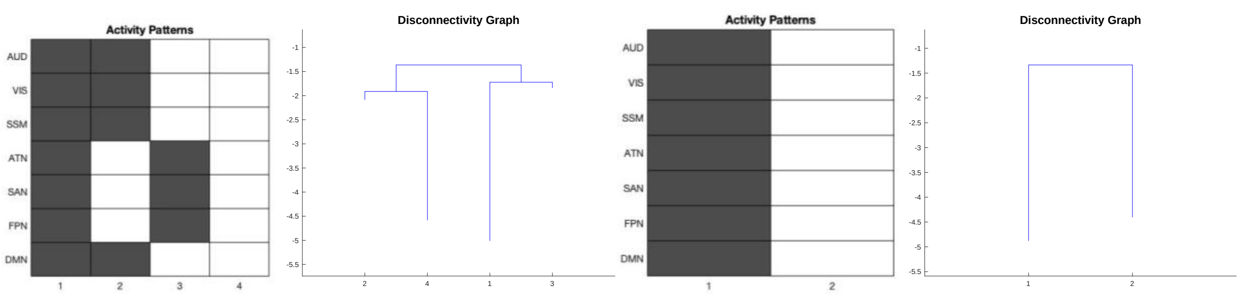

(a) **(b)**

Figure 8: Activity Patterns and Disconnectivity Graph for 7 inter-networks of (**a**) all the averaged controls (**b**) all the averaged patients.

minima. There are 2 identifiable states that are local minima in the SAN region for both SZ and HC subjects. For the SSM region, HC have 3 states that have been identified as local minima, whereas SZ has 2 states identified as local minima. For the VIS region, HC have 2 states that have been identified as local minima, whereas SZ has 3 states identified as local minima.

4. DISCUSSION

4.1 Connectivity States

The internetwork results show that DMN and ATN are strongly decoupled for the HC group. Whereas for SZ, there is a high probability that ATN and DMN are not decoupled. This may suggest that patients who have hallucinations never have a decoupled state. For HC, the probability that ATN and DMN are not decoupled is low, since anticorrelation occurs more frequently.

The intra-network results show that in the ATN region, MTG and STG are coupled and there is more brain flexibility in HC than in SZ. The STG and pSTS in ATN have mostly decoupled states. For both SZ and HC subjects, the AUD, DMN and SAN regions shows all coupled states are working together.

For the FPN region, IPL (body image and perception) is related to IFG (manipulation) through the caudal area, which is related to language due to the temporal region. The SZ separate language processing and other manipulation. The region to process language and region to process motor/planning are separated in SZ. The HC stably separated these regions. SZ formed a stable state to separate regions that process motor/planning and region that process language.

The SSM region explains free will – the ability or inability to control actions. The HC can separate these states, but SZ cannot. In order to separate, one must have awareness and training, and self-awareness is the hallmark of HC. Consistent training helps to form a local minimum which represent habits, thus controlling behavior. Local minima respond to stimulus to make a decision. Local minima could change depending on the response.

In the VIS region, SZ have reproducibility. The different separation between SZ and HC suggests that lower-level visual processing and higher-level visual processing (interpretation, planning, reaction) are separated for SZ, whereas HC are mixing them together.

5. CONCLUSION

Energy landscape analysis technique has been employed to identify brain connectivity biomarkers to separate SZ patients and normal control subjects. Potential biomarkers were identified and their corresponding meanings were interpreted, showing that the analysis technique is an effective method for brain connectivity biomarker extractions.

ACKNOWLEDGMENTS

This research was supported by the NSF grant ECCS-1631820, NIH grants MH112180, MH108148, MH103222, and a Brain and Behavior Research Foundation grant.

REFERENCES

1. Acheson, D. J. and Hagoort, P., "Stimulating the brain's language network: syntactic ambiguity resolution after TMS to the inferior frontal gyrus and middle temporal gyrus," Journal of Cognitive Neuroscience, 25(10), 1664–1677, (2013).
2. Astafiev, S. V., Stanley, C. M., Shulman, G. L., and Corbetta, M., "Extrastriate body area in human occipital cortex responds to the performance of motor actions," Nature Neuroscience, 7(5), 542-548, (2004).
3. Baldo, J. V. and Dronkers, N. F., "The role of inferior parietal and inferior frontal cortex in working memory," Neuropsychology, 20(5), 529–538, (2006).
4. Buchsbaum, B. R., Hickok, G., and Humphries, C., "Role of left posterior superior temporal gyrus in phonological processing for speech perception and production," Cognitive Science, 25(5), 663-678, (2001).
5. Davey, J., Thompson, H. E., Hallam, G., Karapanagiotidis, T., Murphy, C., Caso, I. D., Krieger Redwood, K., Bernhardt, B. C., Smallwood, J., and Jefferies, E., "Exploring the role of the posterior middle temporal gyrus in

semantic cognition: Integration of anterior temporal lobe with executive processes," NeuroImage, 137, 165-177, (2016).
6. Devlin, J. T., Jamison, H. L., Gonnerman, L. M., and Matthews, P. M., "The Role of the Posterior Fusiform Gyrus in Reading," Journal of Cognitive Neuroscience, 18(6), 911-922, (2006).
7. Eckert, M. A., Cute, S. L., Vaden, K. I., Kuchinsky, S. E., and Dubno, J. R., "Auditory Cortex Signs of Age-Related Hearing Loss," Journal of the Association for Research in Otolaryngology, 13(5), 703-713, (2012).
8. Ezaki, T., Watanabe, T., Ohzeki, M., and Masuda, N., "Energy landscape analysis of neuroimaging data," Philosophical Transactions of the Royal Society A: Mathematical, Physical and Engineering Sciences, 375(2096), (2017).
9. Fan, L., Li, H., Zhuo, J., Zhang, Y, Wang, J., Chen, L., Yang, Z., Chu, C., Xie, S., Laird, A.R., Fox, P.T., Eickhoff, S.B., Yu, C., and Jiang, T., "The Human Brainnetome Atlas: A New Brain Atlas Based on Connectional Architecture," Cerebral Cortex, 26(8), 3508-3526, (2016).
10. Fliessbach, K., Weis, S., Klaver, P., Elger, C., and Weber, B., "The effect of word concreteness on recognition memory," NeuroImage, 32(3), 1413-1421, (2006).
11. Friederici, A.D., "The Brain Basis of Language Processing: From Structure to Function," Physiological Reviews, 91(4), 1357-1392, (2011).
12. Grill-Spector, K., Kourtzi, Z., and Kanwisher, N., "The lateral occipital complex and its role in object recognition," Vision Research, 41(10-11), 1409-1422, (2001).
13. Kamali, A., Sair, H. I., Radmanesh, A., and Hasan, K. M., "Decoding the superior parietal lobule connections of the superior longitudinal fasciculus/arcuate fasciculus in the human brain," Neuroscience, 277, 577-583, (2014).
14. Hocking, J., and Price, C. J., "The Role of the Posterior Superior Temporal Sulcus in Audiovisual Processing," Cerebral Cortex, 18(10), 2439-2449, (2008).
15. Huk, A. C., Dougherty, R. F., and Heeger, D. J., "Retinotopy and Functional Subdivision of Human Areas MT and MST," The Journal of Neuroscience, 22(16), 7195-7205, (2002).
16. Koyama, M. S., O'Connor, D., Shehzad, Z., and Milham, M. P., "Differential contributions of the middle frontal gyrus functional connectivity to literacy and numeracy," Scientific Reports, 7(1), (2017).
17. Malach, R., Reppas, J. B., Benson, R. R., Kwong, K. K., Jiang, H., Kennedy, W. A., Ledden, P. J., Brady, T. J., Rosen, B.R., and Tootell, R. B., "Object-related activity revealed by functional magnetic resonance imaging in human occipital cortex," Proceedings of the National Academy of Sciences, 92(18), 8135-8139, (1995).
18. Nordhjem, B., Curcic-Blake, B., Meppelink, A. M., Renken, R. J., de Jong, B. M., Leenders, K. L., van Laar, T., and Cornelissen, F. W., "Lateral and Medial Ventral Regions Interact During the Recognition of Images Revealed from Noise," Frontiers in Human Neuroscience, 9(67), (2016).
19. Pollatos, O., Schandry, R., Auer, D. P., and Kaufmann, C., "Brain structures mediating cardiovascular arousal and interoceptive awareness," Brain Research, 1141, 178-187, (2007).
20. Posner, M. I., Rothbart, M. K., Sheese, B. E., and Tang, Y., "The anterior cingulate gyrus and the mechanism of self-regulation," Cognitive, Affective, & Behavioral Neuroscience, 7(4), 391-395, (2007).
21. Preusser, S., Thiel, S. D., Rook, C., Roggenhofer, E., Kosatschek, A., Draganski, B., Blankenburg, F., Driver, J., Villringer, A., and Pleger, B., "The perception of touch and the ventral somatosensory pathway," Brain, 138(3), 540-548, (2014).
22. Radziunas, A., Deltuva, V. P., Tamasauskas, A., Gleizniene, R., Pranckeviciene, A., Petrikonis, K., and Bunevicius, A., "Brain MRI morphometric analysis in Parkinson's disease patients with sleep disturbances," BMC Neurology, 18(1), (2018).
23. Rangaprakash, D., Deshpande, G., Daniel, T. A., Adam M. Goodman, A. M., Robinson, J. L., Salibi, N. Katz, J. S., Denney, T. S., Jr., and Michael N. Dretsch, M. N., "Compromised hippocampus-striatum pathway as a potential imaging biomarker of mild traumatic brain injury and posttraumatic stress disorder," Human Brain Mapping, 38(6), 2843–2864, (2017).
24. Silvanto, J., Schwarzkopf, D. S., Gilaie-Dotan, S., and Rees, G., "Differing causal roles for lateral occipital cortex and occipital face area in invariant shape recognition," European Journal of Neuroscience, 32(1), 165-171, (2010).
25. Subbaraju, V., Sundaram, S., and Narasimhan, S., "Identification of lateralized compensatory neural activities within the social brain due to autism spectrum disorder in adolescent males," European Journal of Neuroscience, 47(6), 631-642, (2017).
26. Sundermann, B. and Pfleiderer B., "Functional Connectivity Profile of the Human Inferior Frontal Junction: Involvement in a Cognitive Control Network," BMC Neuroscience, 13(1), (2012).

27. Tootell, R. B., Reppas, J. B., Kwong, K. K., Malachi, R., Born, R. T., Brady T. J., Rosen, B. R., and Belliveau, J. W., "Functional analysis of human MT and related visual cortical areas using magnetic resonance imaging," The Journal of Neuroscience, 15(4), 3215-3230, (1995).
28. Torres, E., and Beardsley, S., "Cerebellar Source Localization using Event-Related Potentials in a Simple Motor Task," 2019 9th International IEEE/EMBS Conference on Neural Engineering, (2019).
29. Torrey, E. F., "Schizophrenia and the inferior parietal lobule," Schizophrenia Research, 97(1-3), 215-225, (2007).
30. Tosoni, A., Pitzalis, S., Committeri, G., Fattori, P., Galletti, C., and Galati, G., "Resting-state connectivity and functional specialization in human medial parieto-occipital cortex," Brain Structure and Function, 220(6), 3307-3321, (2014).
31. Uddén, J., Snijders, T. M., Fisher, S. E., Hagoort, P., "A common variant of the CNTNAP2 gene is associated with structural variation in the left superior occipital gyrus," Brain and Language, 172, 16-21, (2017).
32. Vogt, B. A., "Pain and emotion interactions in subregions of the cingulate gyrus," Nature Reviews Neuroscience, 6(7), 533-544, (2005).
33. Wade, A. R., Brewer, A. A., Rieger, J. W., and Wandell, B. A., "Functional measurements of human ventral occipital cortex: Retinotopy and color," Philosophical Transactions of the Royal Society of London. Series B: Biological Sciences, 357(1424), 963-973, (2002).
34. Yousry, T. A., Schmid, U. D., Alkadhi, H., Schmidt, D., Peraud, A., Buettner, A., and Winkler, P., "Localization of the motor hand area to a knob on the precentral gyrus. A new landmark," Brain, 120(1), 141-157, (1997).